

CHARACTERIZATION OF HYDROXYETHYLCELLULOSE-GELATIN BASED COMPOSITES

RAMAZAN BERKER DEMİRAL,* ORÇUN ÇAĞLAR KURTULUŞ** and SEDAT ONDARAL***

*Department of Biomedical Equipment Technology, Tosya Vocational School, Kastamonu University, 37300-Tosya, Kastamonu, Turkey

**Department of Materials and Material Processing Technology, Tosya Vocational School, Kastamonu University, 37300-Tosya, Kastamonu, Turkey

***Department of Forest Products Engineering, Faculty of Forestry, Karadeniz Technical University, 61000-Trabzon, Turkey

✉ Corresponding author: O. Ç. Kurtuluş, ckurtulus@kastamonu.edu.tr

Received July 12, 2024

Hydroxyethyl cellulose–gelatin (HEC-GEL) based aerogels were produced by mixing different ratios of cellulose ether (HEC) with gelatin (GEL) (100%, 80/20%, 50/50%, and 20/80%), and using the lyophilisation technique. CaCl₂ was used as crosslinker (C) to increase the reaction of HEC with GEL. The density, porosity, liquid absorption rates for water, PBS (phosphate buffered saline), methylene blue (MB), and Congo red (CR), as well as water vapor transmission (WVT) and BET-specific surface area of the prepared aerogels were investigated. Also, the materials were characterized by FTIR and SEM, and in terms of their antibacterial activity. All aerogels, both with crosslinker and without, had low density values, in the range of 0.01-0.02 g/cm³. High porosity values were determined for the 100% GEL-C of 98.2% and for 20% HEC-80% GEL of 99.8%. The liquid absorption performance of the aerogels, both with crosslinker and without, showed higher values with a higher amount of GEL added into the formulation. The addition of the crosslinker into the HEC-GEL matrix caused minor changes in chemical composition. This simple lyophilization technique provided almost homogenous compositions, yielding highly porous materials that can be used in different application areas, where high porosity is required.

Keywords: hydroxyethyl cellulose, gelatin, calcium chloride, aerogel

INTRODUCTION

Hydroxyethyl cellulose – HEC – is a cellulosic derivative that is mainly known for having highly hydrophilic and nonionic characteristics, in addition to being biodegradable and biocompatible (Fig. 1a). The basic production process of HEC is a reaction between alkali cellulose and ethylene oxide or chloroethanol, after pretreatment with sodium hydroxide. At the end of the etherification mechanism, hydrogen atoms present in the cellulosic backbone are replaced with hydroxyethyl groups. Due to its nonionic character and solubility in both hot and cold water, HEC is biocompatible with surface-active materials, different polymers, and salts.¹⁻³ Due to its high solubility, it can be prepared with various viscosity. Its large number of -OH and -COOH groups give this polymer the critical property of being able to store a large amount of water in its own structure. Due to its properties, HEC has many

applications, especially in the food and painting industries, where it can be used as thickener, emulsifier, suspender, binder, stabilizer, dispersant *etc.*^{4,5} Also, it has been used in ink applications,⁶ finishing of textile products,⁷ food packaging,⁸ oil and gas industries,⁹ drug delivery,¹⁰ tissue engineering,^{11,12} wound dressings¹³ *etc.*

Gelatin – GEL – is a hydrolysis product of collagen, which is the main component of cartilage, connective tissue, skin, and bone tissues (Fig. 1b).¹⁴ It has a protein content of 85-92%, mineral salts of 2-4%, and water of 8-12%.^{15,16} It has weak polyampholyte specifications and is made up of 13% positive group (lysine and arginine), 12% negative group (glutamic acid and aspartic acid), and 11% hydrophobic structure.¹⁵ The main production process starts with acidic or alkaline pretreatment of collagen to remove impurities from animal skin or bones. Then, its

triple helical conformation is disturbed¹⁶⁻¹⁸ and as a result, two kinds of industrial-grade gelatin are prepared, called type A (acidic pretreatment, isoelectric point of pH 8-9) and type B (alkali pretreatment, isoelectric point of pH 4-5). The molecular weight of these polymers is between 10000 and 400000 g/mol. Due to its characteristics, such as being a biocompatible and biobased polymer, having a low antigenic effect, having a low production cost, easy processing and high level of purity, an amphoteric character, and being easy to modify, it has been used in many different application areas, such as in the foods¹⁹ and food packaging industries,²⁰ cosmetics,²¹ photography,²² pharmaceuticals,²³ and biomedical.^{24,25}

Rapid advancements in materials science have led to the development of highly porous, low-density materials in the form of foams, aerogels, and hydrogels, utilizing both synthetic and natural polymers. Aerogels were first investigated by Kistler and are basically produced by removing the liquid fraction of the gelous phase by different techniques, including lyophilization, vacuum drying, and supercritical drying.²⁶⁻²⁸ The material has a rigid three-dimensional structure, low density

(0.003-0.500 g/cm³), and high porosity (80%-99.8%), which made it highly attractive for many different uses, from catalysts,²⁹ to tissue engineering materials.^{30,31} A cellulose derivative (HEC) was often reported to be used as a component in different formulations of composites in the development of films²² and hydrogels.³²⁻³⁴

Our literature review revealed that, although there are studies on HEC-GEL-based materials, to the authors' knowledge, no detailed characterization of HEC-GEL-based aerogels has been found, specifically when crosslinked with CaCl₂. Therefore, this study primarily aims to identify the characteristics of aerogels based on HEC-GEL, both with and without crosslinker addition, which may be useful for various application areas. Aerogels were produced by mixing HEC with GEL in different ratios, with or without CaCl₂ crosslinker, and then investigated in terms of their liquid absorption (water, PBS, MB, and CR dyes), density and porosity, water vapor permeability, BET surface area, and antibacterial activity. Chemical changes were analysed by FTIR spectroscopy and morphological analysis was performed by SEM.

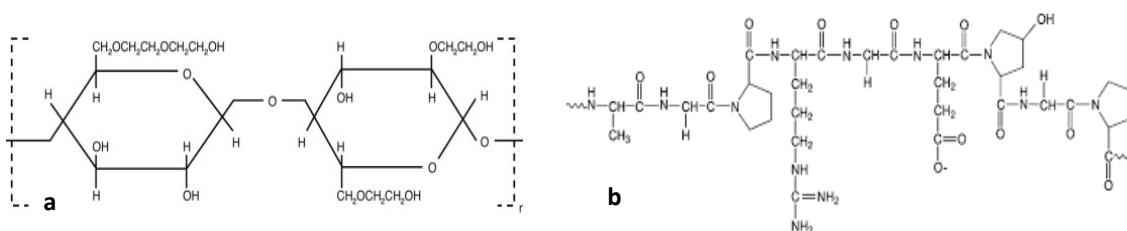


Figure 1: Chemical structure of HEC (a) and GEL (b)^{14,35}

EXPERIMENTAL

Materials

Hydroxyethyl cellulose (HEC) was purchased from Sigma-Aldrich Chemie GmbH (Taufkirchen/Germany), and gelatin (GEL), (obtained from bovine skin; composed of 83-90% protein, 8-12% water, and salts) was kindly provided by Yiğitoğlu Chemical Industry (Istanbul/Turkey). CaCl₂ used as crosslinker, as well as MB and CR dyes (1% stock solution), were purchased from TEKKİM Chemicals Inc. (Istanbul-Turkey). The components for the PBS solution: NaH₂PO₄, KH₂PO₄ and NaCl were purchased from Merck KGaA (Darmstadt/Germany). Deionized water was used during all experiments.

Methods

Preparing HEC, GEL and PBS solutions

Both stock solutions of HEC and GEL were prepared by adding 1 g of polymer to water for a total

volume of 100 mL. The HEC solution was mixed by a magnetic stirrer for 24 hours. The GEL stock was prepared at 35-40 °C by mixing at a 400-450 rpm mixing rate for 40 min, and the solution was used immediately after the production process due to the high gelling capacity.

The PBS stock solution was prepared by mixing 0.2M NaH₂PO₄, 0.2M KH₂PO₄, and 0.15M NaCl. After preparation and before use, the pH of the solution was determined.

Aerogel production

The fundamental solvent casting technique was used to create both pure and crosslinked aerogels. GEL was added to the HEC solution in mixing ratios of 80%-20%, 50%-50%, and 20%-80%, after 1% concentrated polymeric solutions were obtained. For comparison purposes, 100% pure polymers were also prepared. Aerogels containing crosslinker were prepared by the

same method, with the exception that 1% CaCl₂/g HEC was added to the mixing compound immediately after mixing both polymer solutions. HEC-GEL and the pure polymeric solutions were stirred by a mechanical stirrer at 300 rpm for 3 hours, and gelous forms, with homogenous structures, were poured into glass Petri dishes and cooled at -86 °C for 48 hours in a deep freezer. At last, samples were lyophilized at -55 °C and 50 mbar vacuum for 48 hours.

The samples were denoted in accordance with their composition: HEC and GEL (pure polymers), HEC-C and GEL-C (100% of the respective polymer crosslinked with 1% CaCl₂), 80-20, 50-50 and 20-80 (samples with the corresponding ratio of the two polymers), 80-20-C, 50-50-C and 20-80-C (samples with the corresponding ratio of the two polymers crosslinked with 1% CaCl₂).

Determination of density and porosity

The basic method of converting the volume fraction to the weight fraction was used to calculate the density values. Aerogels were weighed for this purpose, and the volume fraction was calculated by measuring their thickness and radius with a micrometer and caliper, respectively. The measured weight was converted to cylindric volume, and density values were calculated. Porosity values of aerogels were determined by using a Helium Pycnometer (Quantachrome Ultrapyc 1200E) and calculated according to Equation (1):

$$\text{Porosity (\%)} = \frac{[V_1 - V_2]}{V_1} \times 100 \quad (1)$$

where V₁: measured density (cm³) and V₂: densities obtained by the pycnometer (cm³).

Water, PBS absorption and dye adsorption capacity

Liquid absorption capacity is an important factor for porous materials, such as aerogels, foams, membranes, and films. For this purpose, water, PBS and dye adsorption values were determined. Briefly, a 0.005 g aerogel sample was prepared and put into a beaker containing 50 mL of deionized water at room conditions. After 24 hours, the aerogels were stabilized by removing excess water with coarse paper, and then weighed. The PBS absorption capacity of the aerogels was also determined by using the same method as for water absorption.

$$\text{Liquid absorption capacity (\%)} = \frac{[M_t - M_o]}{M_o} \times 100 \quad (2)$$

where M_t is the weight of the aerogel after swelling in liquid for 24 h (g), and M_o is initial dry weight of the aerogel (g).

The dye adsorption capacities of the aerogels were determined according to the method proposed by Huang *et al.*³⁶ Approximately 0.025 g of the sample was weighed and placed in 10 mL of dye (MB or CR), with a concentration of 0.5 g/L, with stirring at 200 rpm for 24 h. Dye concentrations were determined by means of a UV-vis spectrophotometer (Shimadzu UV Pharmspec 1700) at different wavelengths. Dye

adsorption capacities of the samples were calculated according to Equation (3):

$$\text{Dye adsorption capacity (mg/g)} = \frac{[C_o - C_e]}{m} \times V \quad (3)$$

where C_e is the equilibrium concentration of the dye solution (mg/L), C_o: the initial concentration of the dye solution (mg/L), m: the weight of the adsorbent used (g), V: the volume of the working solution (L).

BET (Brunauer Emmett Teller) surface area

BET surface area of the aerogels was determined by using the Quantachrome Nova Touch LX4 apparatus. The prepared samples were first subjected to a vacuum for 10 hours at 80 °C to remove excess water and dry the samples completely. According to adsorption-desorption isotherms, specific surface area values were determined by using the Brunauer, Emmett, and Teller (1938) method.³⁷

Water vapor transmission (WVT)

WVT tests were performed according to ASTM standard (E 96-90 Procedure D),³⁸ with a slight modification. Glass bottles (8.5 cm height, 1.2 cm width), with 6 mL of deionized water, were used as a template, and the samples were stuck tightly on the top of the bottles, and then introduced into a dessicator, which comprised saturated MgCl₂·6H₂O and provided 40% humidity. The dessicator was then introduced into an autoclave at 37 °C for 24 hours. The setup, comprising the bottles containing water and the samples, was weighed, and then permeability was calculated according to Equation (4):

$$\text{Water Vapor Transmission Rate} = \frac{(G/t)}{A} \quad (4)$$

where G/t is the slope of the weight change *versus* time (g/h), and A: test area (m²).

FTIR spectroscopy

Chemical characterization of functional groups in aerogels with different compositions, as well as of the pure polymeric materials, was performed by using a Bruker Alpha II FTIR (Billerica/Massachusetts, A.B.D.). Spectra were recorded by scanning 16 scans in the range of 400-4000 cm⁻¹ at 2 cm⁻¹ resolution.

Antibacterial activity

The antibacterial characteristics of the aerogels were determined using the disc diffusion method. *E. coli* grown in SS (Salmonella Shigella Agar) and *S. aureus* grown in BHI (Brain Heart Infusion) enriched media were transferred to agar media via the swap procedure. Following this, a sample of 1 cm diameter was placed in contact with the bacterial habitat. The medium was incubated at 28 °C for 24 hours, after which the inhibition zones associated with bacterial growth in the agar medium were measured and averaged from different sites.

SEM microscopy

SEM images of aerogels were taken with an FEI Quanta FEG 450 (USA) at various magnifications to explore the morphological characteristics of both the surface and cross-sections of the samples. A scalpel was used to cut test samples without disturbing the material structure. A Cressington Spray Coater (Ted Pella Inc., USA) was used to coat sample surfaces with gold-palladium (40 mA current, 50 mbar pressure).

RESULTS AND DISCUSSION**Density and porosity**

Density and porosity are basic properties of porous materials, such as foams, aerogels, films, and membranes. The obtained density and porosity values of all aerogels were listed in Table 1. According to the data, density values were determined between 0.0121 and 0.0195 g/cm³, but the maximum density value was recorded for HEC-C (100% HEC crosslinked with 1% CaCl₂) as 0.0195 g/cm³, and the minimum value – for 20%HEC-80%GEL-C (20-80-C) as 0.0121 g/cm³.

In addition to density, Table 1 also shows the porosity values of aerogels, which were determined to be between 98.2 and 99.8%. The 20-80 composition of the aerogel had the highest porosity value, while GEL-C aerogel had the lowest degree of porosity. It can be seen from the data that the addition of crosslinker to the composition caused a small increase in density values, and at the same time, a slightly decreasing trend for porosity values, especially for pure polymeric aerogels.

The addition of high amounts of GEL to HEC formulations, without crosslinker, clearly increased the porosity values. This situation is probably due to chemical interaction between HEC's OH groups and GEL's cationic reactive groups, which will be seen in FTIR spectra as a

decreasing of the characteristic band intensities of HEC (1640 cm⁻¹) and GEL (1625 cm⁻¹), as will be further discussed below. This interaction probably increased the chemical attack between the reactive sites of the polymers, resulting in much larger pore sizes formed in the materials during the lyophilization. In contrast, the addition of CaCl₂ as a crosslinker caused almost the opposite behavior in terms of porosity, due to the interaction of Ca²⁺ with both the -OH groups of HEC and the anionic sites of GEL. As a result, the unreacted groups of both GEL and HEC molecules behaved as free blocks and filled the main skeleton, resulting in a lower degree of porosity.

Similar results to those reported here regarding density and porosity were obtained by Simon-Herrero *et al.*³⁹ In their research, HEC-alumina-based aerogels were prepared as lightweight insulation materials, and the addition of HEC to the alumina composition caused a decrease in porosity, in contrast to an increase in density.

BET surface area

Aerogels are classified as low-density, highly porous materials in addition to having high specific surface area values. Specific surface area data are given in Table 1, and according to the results, it can be seen that all the aerogels show high surface area values, ranging between 263.13 m²/g and 340.17 m²/g. The highest value was observed for GEL, and the minimum value – for the HEC-C sample. In general, pure HEC samples, with or without crosslinker, showed lower surface area values than GEL samples. Thus, the addition of GEL into HEC composition clearly increased the surface area values.

Table 1
Density, porosity and specific surface area values of aerogels

Sample	Density (g/cm ³)	Porosity (%)	Surface area (m ² /g)
HEC	0.0187	99.50	280.02
GEL	0.0122	98.90	340.17
HEC-C	0.0195	99.01	263.13
GEL-C	0.0125	98.2	313.80
80-20	0.0176	99.60	291.22
50-50	0.0148	99.73	298.56
20-80	0.0124	99.80	305.22
80-20-C	0.0193	99.40	289.23
50-50-C	0.0146	99.20	296.73
20-80-C	0.0121	98.92	299.60

Low density and high porosity are essential in different usage areas of related materials, such as adsorbents, dust collectors, biomaterials, *etc.* In biomedical devices, such as hemostatic agents, wound dressings, and tissue scaffolds, a high surface area is mandatory, for promoting the attachment and proliferation of new tissue cells during the healing process. Similarly, high porosity is imperative in adsorbents. For example, Gao *et al.* prepared HEC-silica-graphitic carbon nitride-based foams and used the freeze-drying technique, with and without a gas foaming process, for obtaining a porous material to be used for dye adsorption.⁴⁰ High dye adsorption was recorded for both non-gas foamed (HEC/SiO₂/C₃N₄-50) and gas foamed (HEC/SiO₂/C₃N₄-80) samples, which showed surface areas of 38 and 47 m²/g, respectively. Although both silica and graphitic carbon nitride have higher specific surface areas, the samples prepared with HEC had low surface area values.

Salerno *et al.* produced GEL-based porous composites by using type A and type B gelatin, by the combined sol-gel technique and sCO₂ drying, with/without crosslinker 3-glycidoxypropyltrimethoxysilane (GOTMS). According to the obtained results, the highest specific surface area values were achieved by the addition of 30% GOTMS for type A and type B-based samples – of approximately 150 and 70 m²/g, respectively; while those for the pure GEL were ~20 m²/g and ~60 m²/g for type B and type A GEL, respectively.⁴¹ The highly different surface area values reported in the described study and in this work can be explained by the difference in the characteristics of the materials and the reaction mechanisms between the components.

Water, PBS and dye adsorption performance

The absorption performance of the aerogels produced with/without crosslinker towards water and PBS is illustrated in Figure 2 (a-b), which reveals a high absorption capacity of the samples. The maximum liquid absorption performance was recorded for the 20-80 samples, as 966% and 550% for water and PBS, respectively. It should be noted that no absorption value could be determined for the pure GEL composite because of its fast dissolution in both liquid media. This situation can be explained by the fact that GEL is a highly hydrophilic material and easily dissolves in these media. However, the addition of GEL to the HEC for a composite formulation clearly improved liquid absorption at a higher level, compared to that

of the pure HEC sample due to GEL's hydrophilicity. Moreover, porosity values also explain the aerogels' liquid absorption behavior. Increasing amounts of GEL in the HEC matrix generally provide increasing porosity values, which is a critical factor affecting the absorption behavior of porous materials.

In Figure 2 (b), the liquid absorption (water and PBS) performances of CaCl₂ added aerogels are given. When compared to non-crosslinked samples, it can be clearly seen that both water and PBS absorption values were determined to be lower. Water and PBS absorption values decreased from 700% to 585% and from 450% to 355%, respectively. These results were supported by both porosity and surface area values, which show a clearly decreasing trend with the addition of CaCl₂ to the HEC matrix. The absorption performance of the 100% GEL sample could not be determined, and even the addition of 1% CaCl₂ crosslinker into the composition could not fully prevent the dissolution of GEL. Similarly to the case of non-crosslinked samples, the addition of GEL to the HEC matrix provides increasing absorption values for both water and PBS. A lower absorption degree is an expected result due to the high reactivity between the -OH groups of HEC and the reactive groups of GEL with Ca²⁺ ions, resulting in blocking of the hydrophilic nature of both polymers. This situation is clearly in agreement with the porosity and surface area results of all the samples, where crosslinked samples had lower porosity and surface area values. In addition to testing the adsorption of the aerogels towards water and PBS, two different dyes (MB and CR) were also used to characterize the aerogels' adsorption behavior. Figure 3 shows the results of this test. As seen in the figure, the adsorption behavior of some samples could not be determined because of the high gelation of the samples. The two types of dyes showed different behavior in different composite mixtures. However, high adsorption values were determined for all the composites. The highest MB adsorption value was determined for the 20-80 formulation as 138 mg/g, whereas the lowest value – for the pure GEL sample as 2.22 mg/g. It should be noted that, similarly to the water and PBS tests, GEL behaved in the same manner, meaning that there was high dissolution and gelation in a few minutes, and it was difficult to remove this sample from the dye solution. In contrast to the pure GEL without a crosslinker, the crosslinked GEL sample had a significant level of MB adsorption. This situation clearly shows that the interaction between

GEL and CaCl₂ provides a firmer structure, without decomposition, and this situation resulted in a higher absorption capacity in the pores of the related sample. Although the crosslinked GEL shows a lower degree of porosity and surface area than the non-crosslinked samples, this firm structure ensured higher adsorption towards MB.

When investigating HEC-GEL composites, MB adsorption values show parallel results with porosity changes. A decreasing trend of porosity clearly showed a decreasing trend of MB

adsorption. Similar to the results of this study, it was reported previously for HEC-silica-carbon nitride foams produced with high porosity and pore volume, which led to high adsorption values, of 132.45 mg/g for MB and 206.62 mg/g for methylene violet.⁴² When compared to our results, it should be stated that the differences in the composition may explain the different liquid adsorption behavior of the materials.

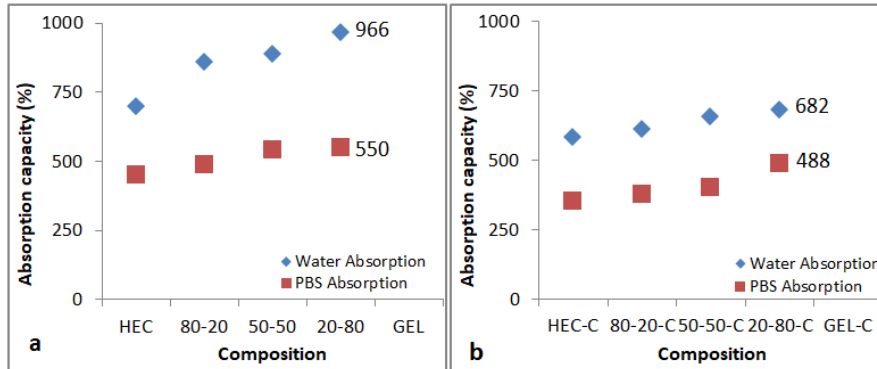


Figure 2: Water and PBS absorption capacity of (a) non-crosslinked, and (b) crosslinked aerogels

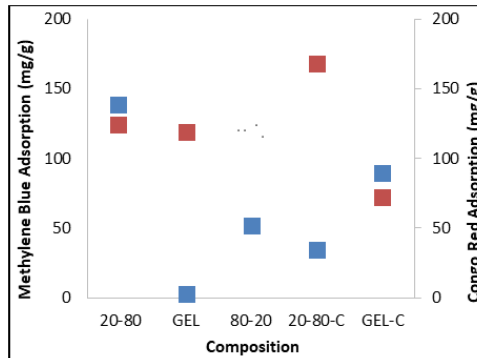


Figure 3: MB (blue symbol) and CR (red symbol) adsorption performance of aerogels

In addition to MB, the CR adsorption capacities of the aerogels were also investigated, and the results are also shown in Figure 3. As mentioned above, the test could be completed for some samples, as they either dissolved or easily turned to a gelous form, and could not be removed from the dye solution. Adsorption values between 72.663 mg/g and 168.268 mg/g were determined. The pure GEL, without crosslinker, had an adsorption performance in the higher range, which can be promoted by the higher reactive components present in GEL molecules. Conversely, the crosslinker blocked the anionic sites easily during aerogel production. As a result, the cationic sites of the GEL molecule showed high efficiency for anionic CR dye. Similar to water and PBS

adsorption results, the 20-80-C sample showed the highest CR adsorption value, and this can be explained by the fact that more cationic sites in GEL's composition probably reacted with the anionic dye and Ca²⁺ ions of the crosslinker reacted with the -OH groups of the HEC molecule.

According to the adsorption results, the aerogels prepared in this study could be suitable for use in different areas where high absorption capacities are needed. Although some formulations have low resistance, such as 100% HEC, 50-50, and their crosslinked samples, it can be assumed that the addition of a higher amount of crosslinker will probably promote higher resistance and lower absorption values, according to our results.

Water vapor transmission (WVT)

Another important characteristic of porous materials is water vapor transmission. This property is mainly affected by the pore volume, pore diameter, porosity, specific surface area values, and crystalline structure of polymers. In Figure 4 (a-b), the WVT results for non-crosslinked and crosslinked aerogels are presented. As may be noted, the results range between 155.4 and 256.69 g/m² h, where the maximum value was obtained for the composite with a higher amount of GEL in the HEC matrix (20-80). The high porosity and surface area values obviously lead to higher vapor transmission in 24 hours for this formulation. Although the porosity and surface

area values of the 80-20 sample increased, as compared to the pure HEC sample, the WVT result revealed a nearly negligible decreasing trend. When the level of GEL in the primary matrix is increased, there is an increasing trend of WVT, which is caused by the wide surface area and high porosity values. Furthermore, the high hydrophilic nature of GEL may explain why it has a lower WVT than pure HEC, as high moisture content (40%) during the test may promote the gelation of GEL and the pores of the material collapsed and were closed by GEL. As a result, vapor transmission through the sample was retarded.

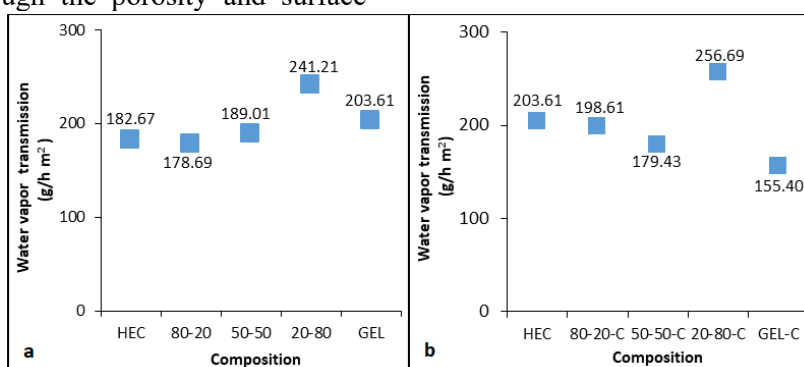


Figure 4: Water vapor transmission results of non-crosslinked (a) and crosslinked (b) aerogels

In Figure 4 (b), the WVT results of crosslinked aerogels are given. Similarly to the non-crosslinked materials, the highest value was observed for the 20-80-C sample – of 256.69 g/h m². Also, it is clear that the pure GEL sample had a higher WVT than the crosslinked GEL sample, which can be clearly correlated with the decrease in both porosity and surface area value with the addition of crosslinker. However, a lower value was also observed for 50-50-C, compared to the non-crosslinked sample. This situation is also likely caused by the nature of the pure GEL, which led to decreasing porosity and surface area values. According to our results, this material has quite high WVT results.

The WVT of different composites with different physical forms has been investigated in the literature. Bioplastic films with HEC and HEC-polyvinylpyrrolidone (HEC-PVP) mixtures were produced by Anwar *et al.* (2024), and their WVT were found as 91.91 g/m² h and 91.93 g/m² h for pure HEC and HEC-PVP 5:3, respectively.⁴³ Compared to the mentioned study, higher WVT results for pure HEC in this work are probably due to the differences in the micromorphological structure. As known, aerogels and foams have

highly porous structures due to interconnected pores, which provide holes through the main skeleton; however, films and membrane structures are compressed and packed densely. The results obtained in our study show that the developed materials could be promising for areas where high WVT values are required, such as in wound dressings, but for such uses the materials need to be subjected to biocompatibility tests.^{44,45}

FTIR analysis

Chemical changes during the preparation of composites have been investigated by FTIR spectroscopy. The FTIR spectra of non-crosslinked and crosslinked aerogels, in addition to those of pure polymeric samples, are shown in Figure 5. In Figure 5 (a), FTIR spectrum of pure HEC shows characteristic peaks at 3397 cm⁻¹ and 2871 cm⁻¹ associated with the H stretching vibrations of -OH groups and C-H groups, respectively.⁴⁶ Additionally, the peaks at 1641 cm⁻¹, 1064 cm⁻¹ and 1015 cm⁻¹ are associated with glucose ring tension, C-O interaction, and tension vibration of C-OH groups.⁴⁶⁻⁴⁸ The main characteristic peaks of gelatin normally occur at 1631 cm⁻¹, 1530 cm⁻¹ and 1229 cm⁻¹, being associated with C=O stretching

vibration of amide-I, N-H bending vibration of amide-II, and C-N stretching vibration, respectively. In this study, the spectrum of the pure GEL sample shows these peaks at 1635 cm^{-1} , 1543 cm^{-1} and 1237 cm^{-1} , respectively.^{50,51} When analyzing all the spectra in Figure 5 (a), the characteristic peak of GEL at 1625 cm^{-1} is clearly seen in all compositions at different intensities.

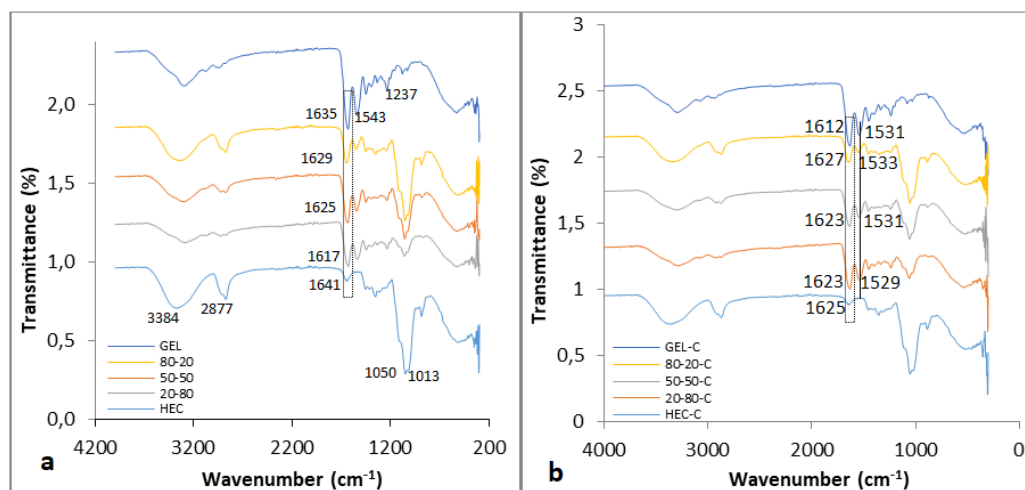


Figure 5: FTIR spectra of (a) non-crosslinked, and (b) crosslinked aerogel samples

The FTIR spectra of crosslinked aerogels presented in Figure 5 (b) show similar peak behavior to that of non-crosslinked samples, with different peak intensities. The reduction of peak intensity of the reactive groups was the most significant modification visible in the FTIR spectra with the addition of the crosslinker. It is noted that the addition of CaCl_2 to the pure polymer samples (HEC and GEL) clearly led to reactions with the active groups of the polymers, as can be observed by the decrease of basic peak intensities that shifted from 1635 cm^{-1} to 1612 cm^{-1} and from 1641 cm^{-1} to 1625 cm^{-1} for GEL and HEC, respectively. This is most probably caused by the reaction of Ca^{2+} ions present in the crosslinker with the -OH groups of HEC and also with the anionic fractions of GEL, such as glutamic and aspartic acids. The FTIR spectra of the composite samples also show the same trend as their corresponding non-crosslinked samples, with decreasing peak intensities in the regions around 1500 and 1620 cm^{-1} . Also, it is clearly seen that the addition of the crosslinker obviously led to lower peak intensities in the region around 1620 cm^{-1} .

Antibacterial efficiency

The antibacterial activity is one of the essential properties of materials that are intended to be used

However, the active peak at 1640 cm^{-1} , which is attributed to HEC, shifted towards 1625 cm^{-1} and lost its intensity. A similar situation is noted in the GEL structure: the 1530 cm^{-1} peak intensities, which correspond to the N-H bending vibration of amide II, varied with the quantity of HEC present. This situation definitely shows the chemical interaction that occurred between polymers.

as wound healing and hemostatic agents, tissue scaffolds, and food packaging systems in the form of films, foams, aerogels, hydrogels, *etc.* The results obtained by the disc diffusion method can be seen in Figure 6. As may be noted, the aerogels had no antibacterial effect on the tested bacterial strains (*S. aureus* and *E. coli*). Moreover, the addition of the crosslinker to the formulation did not provide an antibacterial effect either. It is obvious that both biopolymers were used as raw nutrients by bacteria, as may be remarked by the bacterial colonies that moved toward the center of the samples.

HEC's negative performance against bacteria was also established in a study by Wei *et al.*,⁵¹ in which acrylic acid-N-N' methylene bisacrylamide-based single-stage copolymerization products were produced in a polyhexamethylene-HEC mixture. Results showed that the addition of HEC to polyhexamethylene guanidin hydrochloride, which was used in papermaking, decreased the antibacterial effect when compared to pure polyhexamethylene guanidin hydrochloride.

Also, the lack of antibacterial activity of pure GEL was confirmed by earlier research. For example, Ye *et al.*⁵² developed bacterial cellulose-GEL-based porous sponge materials for wound dressing applications, incorporating the model

drug ampicillin. They showed that the aerogels without the model drug showed no antibacterial activity against *E. coli*, *C. albicans* and *S. aureus*. Other studies also confirmed the need to

incorporate an antibacterial agent into GEL-based formulations in order to obtain an antibacterial performance of the materials.^{53,54}

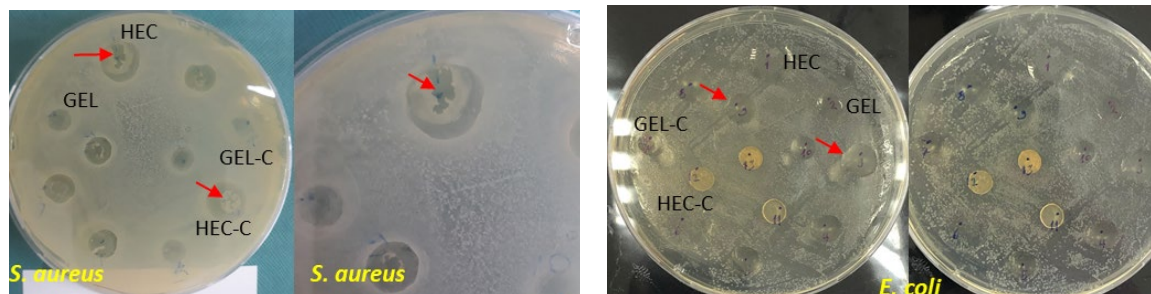


Figure 6: Antibacterial test images for *S. aureus* and *E. coli*

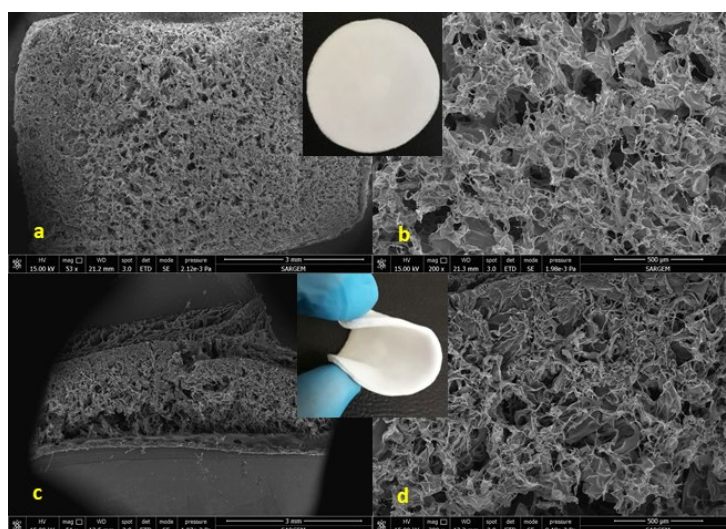


Figure 7: SEM images of pure HEC sample: surface (a-b) and cross-sectional (c-d) views

SEM analysis

Surface and cross-section SEM images of a pure HEC sample are seen in Figure 7. The porous structure of the sample is clearly seen in Figure 7 (a-b), and the network structure of HEC can be identified. SEM images reveal mostly a dense structure, which is in agreement with the porosity values discussed above. Although the sample had a dense and compact structure, it was noted that it had fast liquid absorption. The cross-sectional SEM images in Figure 7 (c-d) shows similar morphology, of a dense structure, with small pores.

In Figure 8, surface and cross-sectional SEM images of HEC-GEL 50-50 formulation, with and without crosslinker, are presented. Surface images of both samples clearly show porous structures;

however, the presence of the crosslinker led to a denser structure, compared to that of the same formulation without crosslinker. This confirms the effect of the crosslinker in the polymer formulation, causing the macromolecular chains of the polymers to interact closer in the HEC-GEL structure. Compared to the pure HEC, the cross-sectional views of the HEC-GEL 50-50 samples revealed some differences. The fast diffusion mechanism occurring during the lyophilization process probably caused this effect, considering that the low-viscosity GEL fraction probably diffused out of the matrix faster. The findings confirm the results for both porosity and surface area discussed earlier in the paper.

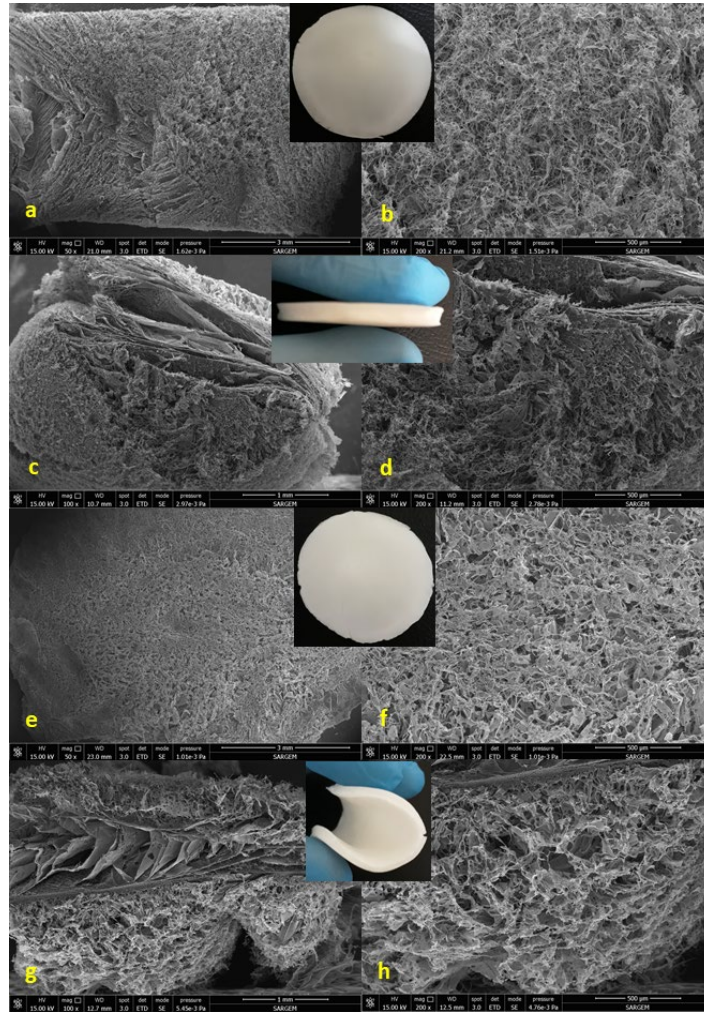


Figure 8: SEM images of HEC-GEL 50-50 (a-d) and 50-50-C (e-h) samples (a, b, e, f – surface views, and c, d, g, h – cross-sectional views)

CONCLUSION

HEC-GEL aerogels were produced by adding varying amounts of GEL into the HEC matrix, with and without the addition of 1% CaCl_2 crosslinker. Samples were produced by the conventional freezing-lyophilization approach. The water, PBS and dye adsorption (MB and CR), WVT, specific surface area and antibacterial activity of the materials were determined. Also, the FTIR spectra and SEM images of the samples were examined. According to the findings, all the aerogels had low density, ranging between 0.0121 g/cm^3 and 0.0195 g/cm^3 , and high porosity values between 98.2-99.8%, which are important characteristics for materials intended for adsorption and biomedical applications. In addition, the samples had high liquid absorption performances for water (700-966% for non-crosslinked, 585-682% for crosslinked), PBS (450-550% for non-crosslinked, 355-488% for crosslinked), and for MB and CR dyes. It should be noted, however, that the integrity

of the materials was affected in some cases for both non-crosslinked and crosslinked samples. FTIR spectra revealed comparable patterns, but the chemical interaction between the biopolymers and the crosslinker was clearly visible by the decrease of the basic peak intensities from 1635 cm^{-1} to 1612 cm^{-1} and 1641 cm^{-1} to 1625 cm^{-1} for GEL and HEC, respectively, with crosslinker addition. The materials had no antibacterial activity in themselves, but their porous structure, as confirmed by SEM, could be helpful for the incorporation of antimicrobial agents. Thus, the prepared aerogels could be promising precursors for the development of advanced materials for application areas where high porosity is required.

ACKNOWLEDGEMENT: The Scientific and Technological Research Council of Turkey (TÜBİTAK) provided financial support to all of the authors within the scope of the Tübitak-2209 project.

REFERENCES

- ¹ D. Wang, E. McLaughlin, R. Pfeffer and Y. S. Lin, *Ind. Eng. Chem. Res.*, **50**, 21 (2011), <https://doi.org/10.1021/ie201301n>
- ² T. Huang, Y. W. Shao, Q. Zhang, Y. F. Deng, Z. X. Liang *et al.*, *ACS Sustain. Chem. Eng.*, **7**, 9 (2019), <https://doi.org/10.1021/acssuschemeng.9b00691>
- ³ F. Ning, J. Zhang, M. Kang, C. Ma, H. Li *et al.*, *J. Appl. Polym. Sci.*, **138**, 8 (2021), <https://doi.org/10.1002/app.49880>
- ⁴ A. G. Dal-Bó, R. Laus, A. C. Felipe, D. Zanette and E. Minatti, *Colloids Surf. A Physicochem. Eng. Asp.*, **380**, 1 (2011)
- ⁵ Y. Hui, R. Liu, L. Li, Q. Sun, Z. Xiao *et al.*, *J. Por. Mater.*, **30**, 1735 (2023), <https://doi.org/10.1007/s10934-023-01458-8>
- ⁶ Y. Liang, X. Liu, K. Fang, F. An, C. Li *et al.*, *Prog. Org. Coat.*, **154**, (2021)
- ⁷ R. K. Nag, A. C. Long and M. J. Clifford, *Conf. Pap. Sci.*, (2013), <https://doi.org/10.1155/2013/956072>
- ⁸ Y. Balçık Tamer, *Polym. Plast. Technol. Eng.*, **62**, 9 (2023), <https://doi.org/10.1080/25740881.2023.2195908>
- ⁹ S. Chen, Q. Shao, L. Hu, Z. Tan and D. Zheng, *J. Water Process.*, **52**, (2023), <https://doi.org/10.1016/j.jwpe.2023.103503>
- ¹⁰ F. Buang, A. Chatzifragkou, M. C. Amin and V. V. Khutoryanskiy, *Polymers*, **15**, 1 (2023), <https://doi.org/10.3390/polym15010093>
- ¹¹ M. Hojabri, T. Tayebi, M. Kasravi, A. Aghdaee, A. Ahmadi *et al.*, *Int. J. Biol. Macromol.*, **240**, 124492 (2023), <https://doi.org/10.1016/j.ijbiomac.2023.124492>
- ¹² K. T. Le, C. T. Nguyen, T. D. Lac, L. G. T. Nguyen, T. L. Tran *et al.*, *J. Drug Deliv. Sci. Technol.*, **82**, 104318 (2023), <https://doi.org/10.1016/j.jddst.2023.104318>
- ¹³ V. Mohammadzadeh, E. Mahmoudi, R. Soghra, N. Maryam, R. A. Taheri *et al.*, *J. Drug Deliv. Sci. Technol.*, **86**, (2023), <http://dx.doi.org/10.2139/ssrn.4409420>
- ¹⁴ M. A. El-Sheikh, S. M. El-Rafie, E. S. Abdel-Halim and M. H. El-Rafie, *J. Polym.*, (2013), <http://dx.doi.org/10.1155/2013/650837>
- ¹⁵ A. Khakalo, I. Filpponen, L. S. Johansson, A. Vishtal, A. R. Lokanathan *et al.*, *React. Funct. Polym.*, **85**, (2014), <https://doi.org/10.1016/j.reactfunctpolym.2014.09.024>
- ¹⁶ R. Schrieber and H. Gareis, "Gelatin Handbook-Theory and Industrial Practice", Wiley-VCH, 2007
- ¹⁷ M. S. Palan Abdullah, M. I. Noordin, S. I. M. Ismail, N. M. Mustapha, M. Jasamai *et al.*, *Sains Malays.*, **47**, 2 (2018), <http://dx.doi.org/10.17576/jsm-2018-4702-15>
- ¹⁸ H. Yetim, "Jelatin Üretimi, Özellikleri ve Kullanımı-1, Ulusal Helal ve Sağlıklı Gıda Kongresi, Gıda Katkı Maddeleri: Sorunlar ve Çözüm Önerileri", 19-20 Kasım 2011, Ankara-Türkiye
- ¹⁹ J. Gómez-Estaca, R. Gavara and P. Hernández-Muñoz, *Innov. Food Sci. Emerg. Technol.*, **29**, (2015), <https://doi.org/10.1016/j.ifset.2015.03.004>
- ²⁰ O. Abdelhedi, A. Salem, R. Nasri, M. Nasri and M. Jridi, *Curr. Opin. Food Sci.*, **43**, (2022), <https://doi.org/10.1016/j.cofs.2021.12.005>
- ²¹ F. Rahmandari, F. Swastawati and R. A. Kurniasih, *IOP Conf. Ser. Earth Environ. Sci.*, **750**, 1 (2021)
- ²² M. E. Osman, S. Ismael, E. Ciliberto, S. Stefani and Y. M. Elsaba, *Int. J. Conserv. Sci.*, **13**, 2 (2022)
- ²³ W. Qu, I. B. Qader and A. P. Abbott, *Drug Deliv. Transl. Res.*, **12**, 5 (2022), <https://doi.org/10.1007/s13346-021-00998-3>
- ²⁴ W. Liang, P. Wu, S. Yan, S. Wang, J. Zhao *et al.*, *Appl. Mater. Today*, **38**, (2024), <https://doi.org/10.1016/j.apmt.2024.102227>
- ²⁵ M. Arumugam, B. Murugesan, P. M. Sivakumar, N. Pandiyan, D. Kumar Chinnalagu *et al.*, *Process Biochem.*, **124**, 221 (2023), <https://doi.org/10.1016/j.procbio.2022.11.019>
- ²⁶ S. S. Kistler, *J. Phys. Chem.*, **36**, 1 (1932), <https://doi.org/10.1021/j150331a003>
- ²⁷ S. S. Kistler, United States Patent No: 2,093,454, Method of Producing Aerogels, 1937
- ²⁸ B. J. C. Duchemin, M. P. Staiger, N. Tucker and R. H. Newman, *J. Appl. Polym. Sci.*, **115**, 216 (2010), <https://doi.org/10.1002/app.31111>
- ²⁹ E. Guilminot, F. Fischer, M. Chatenet, A. Rigacci, S. Berthon-Fabry *et al.*, *J. Power Sources*, **166**, 1 (2007), <https://doi.org/10.1016/j.jpowsour.2006.12.084>
- ³⁰ B. Ş. Ayyvazoğlu, M. Ceylan, A. A. I. Turan and E. B. Yılmaz, *Polymers*, **15**, 9 (2023), <https://doi.org/10.3390/polym15092022>
- ³¹ C. B. Schimper, P. Pachschröll, M. F. Maitz, C. Werner, T. Rosenau *et al.*, *Front. Bioeng. Biotechnol.*, **11**, (2023), <https://doi.org/10.3389/fbioe.2023.1152577>
- ³² P. Chen, X. Liu, R. Jin, W. Nie and Y. Zhou, *Carbohydr. Polym.*, **167**, 36 (2017), <https://doi.org/10.1016/j.carbpol.2017.02.094>
- ³³ T. Peng, J. Zhu, T. Huang, C. Jiang, F. Zhao *et al.*, *J. Appl. Polym. Sci.*, **138**, 23 (2021), <https://doi.org/10.1002/app.50539>
- ³⁴ X. Zhang, T. Zuo, M. Ai, D. Yu and W. Wang, *ACS Sustain. Chem. Eng.*, **12**, 28 (2024), <https://doi.org/10.1021/acssuschemeng.4c02060>
- ³⁵ N. Rong, C. Chen, K. Ouyang, K. Zhang, X. Wang *et al.*, *Sep. Purif. Technol.*, **274**, 119120 (2021), <https://doi.org/10.1016/j.seppur.2021.119120>
- ³⁶ S. Huang, L. Wu, T. Li, D. Xu, X. Lin *et al.*, *Int. J. Biol. Macromol.*, **137**, 234 (2019), <https://doi.org/10.1016/j.ijbiomac.2019.06.234>
- ³⁷ S. Brunauer, P. H. Emmett, E. Teller, *J. Am. Chem. Soc.*, **60**, 2 (1938)
- ³⁸ ASTM E96/E96M-14, Standard Test Methods for Water Vapour Transmission of Materials
- ³⁹ C. Simón-Herrero, A. Romero, J. L. Valverde and L. Sánchez-Silva, *J. Mater. Sci.*, **53**, (2018), <https://doi.org/10.1007/s10853-017-1584-6>
- ⁴⁰ Z. Z. Gao, N. Qi, W. J. Chen and H. Zhao, *Arab. J. Chem.*, **15**, 9 (2022), <https://doi.org/10.1016/j.arabjc.2022.104105>

- ⁴¹ A. Salerno, L. Verdolotti, M. G. Raucci, J. Saurina, C. Domingo, *et al.*, *Eur. Polym. J.*, **99**, 230 (2018), <https://doi.org/10.1016/j.eurpolymj.2017.12.024>
- ⁴² W. C. Lin, C. C. Lien, H. J. Yeh, C. M. Yu and S. H. Hsu, *Carbohydr. Polym.*, **94**, 1 (2013), <https://doi.org/10.1016/j.carbpol.2013.01.076>
- ⁴³ B. Anwar, C. Nurhashiva, W. R. Arwa and G. Yuliani, *J. Serb. Chem. Soc.*, **89**, 2 (2024), <https://doi.org/10.2298/JSC231023103A>
- ⁴⁴ L. Motelica, D. Ficai, G. Petrisor, O. C. Oprea, R. D. Truşcă *et al.*, *Pharmaceutics*, **16**, 9 (2024), <https://doi.org/10.3390/pharmaceutics16091225>
- ⁴⁵ F. Lv, C. Wang, P. Zhu and C. Zhang, *Cellulose*, **21**, (2014), <https://doi.org/10.1007/s10570-014-0440-y>
- ⁴⁶ G. F. El Fawal, M. M. Abu-Serie, M. A. Hassan and M. S. Elnouby, *Int. J. Biol. Macromol.*, **111**, 649 (2018), <https://doi.org/10.1016/j.ijbiomac.2018.01.040>
- ⁴⁷ J. G. Vieira, G. de Carvalho Oliveira, G. Rodrigues Filho, R. M. N. de Assunção, C. da Silva Meireles *et al.*, *Carbohydr. Polym.*, **78**, 4 (2009), <https://doi.org/10.1016/j.carbpol.2009.06.016>
- ⁴⁸ W. Wang, J. Wang, Y. Kang and A. Wang, *Compos. B Eng.*, **42**, 4 (2011), <https://doi.org/10.1016/j.compositesb.2011.01.018>
- ⁴⁹ S. Farris, J. Song and Q. Huang, *J. Agric. Food Chem.*, **58**, 2 (2010), <https://doi.org/10.1021/jf9031603>
- ⁵⁰ Q. Lu, S. Zhang, M. Xiong, F. Lin, L. Tang, B. Huang *et al.*, *Carbohydr. Polym.*, **196**, 225 (2018), <https://doi.org/10.1016/j.carbpol.2018.05.020>
- ⁵¹ D. Wei, Y. Chen and Y. Zhang, *Carbohydr. Polym.*, **136**, 543 (2016), <https://doi.org/10.1016/j.carbpol.2015.09.086>
- ⁵² S. Ye, L. Jiang, C. Su, Z. Zhu, Y. Wen *et al.*, *Int. J. Biol. Macromol.*, **133**, 148 (2019), <https://doi.org/10.1016/j.ijbiomac.2019.04.095>
- ⁵³ A. Mirtaghavi, A. Baldwin, N. Tanideh, M. Zarei, R. Muthuraj *et al.*, *Int. J. Biol. Macromol.*, **164**, 1949 (2020), <https://doi.org/10.1016/j.ijbiomac.2020.08.066>
- ⁵⁴ B. Özkahraman, Z. Özbaş, G. Bayrak, E. Tamahkar, I. Perçin *et al.*, *Int. J. Polym. Mater. Polym. Biomater.*, **71**, 16 (2022), <https://doi.org/10.1080/00914037.2021.1960341>